Thin Solid Films xxx (2014) xxx–xxx

Contents lists available at ScienceDirect

Thin Solid Films

journal homepage: www.elsevier.com/locate/tsf

Adaptation of the surface-near Ga content in co-evaporated Cu(In,Ga)Se_2 for CdS versus Zn(S,O)-based buffer layers

Torben Klinkert *, Thibaud Hildebrandt, Marie Jubault, Frédérique Donsanti, Jean-François Guillemoles, Negar Naghavi

Institute of Research and Development on Photovoltaic Energy (IRDEP) (UMR 7174, EDF/CNRS/Chimie ParisTech), Chatou 78401, France

ARTICLE INFO

Available online xxxx

Keywords:
Copper indium gallium selenide
Buffer layer
Zinc sulfide
Zinc oxysulfide
Composition gradient
Interface
Glow discharge optical emission spectroscopy

ABSTRACT

In this work, we show that in order to optimize the efficiency of Cu(In_{1-x},Ga_x)Se_2 (CIGS) solar cells with Cd-free Zn(S,O)-based buffer layers, the Ga concentration in the CIGS absorber layer towards the hetero-interface has to be adapted. We varied the In and Ga deposition rates in the last stage of our 3-stage co-evaporation process, leading to different compositional ratios x_f = [Ga] / ([Ga] + [In]) between 0.15 and 0.6 in the top 400 nm of the absorber layer. All absorber layers were then completed with both CdS and Zn(S,O) buffer layers by chemical bath deposition. While cells with our standard grading of $x_f \approx 0.4$ in the front region result in a best performance of 15% with a CdS buffer, similar efficiencies with a Zn(S,O) buffer layer are only obtained when the Ga content near the hetero-interface is reduced down to $x \approx 0.25$. The maximum efficiency for the CdS buffer layer coincides with the maximum open circuit voltage (V_{oc}) and fill factor (FF). Interestingly, for the Zn(S,O) buffer layer, this is not the case: the V_{oc} increases steadily for higher Ga ratios, while the FF is fairly constant for $0.25 < x < 0.5$ and decreases drastically for more extreme values. The findings are explained by differences in the conduction band offsets which result from the conduction band shift close to the surface due to Ga content variations. The results illustrate the importance of the absorber layer adaptation for different buffer layers and are an important step on the way to Cd-free buffer layers.

1. Introduction

To date, photovoltaic modules based on Cu(In,Ga)Se_2 (CIGS) have reached the commercialization state and entered the solar cell market. The usual cell structure is glass/Mo/CIGS/CdS/i-ZnO/ZnO:Al. The replacement of the CdS buffer layer is desirable for environmental reasons (toxicity of Cd) as well as for the cell performance (reduction of detrimental absorption in the buffer layer by using higher band gap materials). A comprehensive overview of different buffer layer technologies is given in [1]. The comparison of devices with different buffer layers is also interesting from a scientific point of view. The *p–n* junction formation between the p-type CIGS and the n-type buffer layer is subject to numerous scientific discussions and in the literature different models have been proposed for its explanation. The classic understanding is a hetero junction formation between the two layers and thus energy band discontinuities at the *p–n* interface. For Cu-poor CIGS (y = [Cu] / ([In] + [Ga] < 1), the formation of an n-type, so-called ordered vacancy compound (OVC) layer in the front region of the CIGS layer has been reported, possibly Cu(In,Ga)$_3Se_5$ or Cu(In,Ga)$_5Se_8$ [2–4]. This moves the *p–n* junction away from the CIGS/buffer layer interface into the absorber layer and thus decouples the electronic from the structural junction. More recently, the formation of a buried homo-junction due to the diffusion of n-dopants from the buffer layer (Cd for CdS [5–8] and Zn for Zn(S,O) [9]) into the top part of the CIGS absorber layer or OVC have been reported. In all these scenarios, it is clear that the choice of the buffer layer will play a key role in the junction formation mechanism.

In this work, we regard the interdependence between the choice of the buffer layer (CdS and Zn(S,O)) and the CIGS properties in the near-interface region. While often the Ga concentration in the whole absorber layer is varied [10], we varied the In and Ga deposition rates only during the 3rd stage of our 3-stage co-evaporation process. This way, 7 absorber layers with different Ga contents x_f = [Ga] / ([Ga] + [In]) only in about the top 400 nm were obtained and then each completed both with a CdS and a Zn(S,O) buffer layer. The in-depth Ga gradient was measured by glow discharge optical emission spectroscopy (GD-OES) and the interface near region was investigated by Raman spectroscopy. The observed solar cell parameters are explained in terms of the conduction band (E_C) alignment at the hetero-interface.

2. Experimental

2.1. Absorber layer fabrication

The CIGS absorber layers were deposited in a co-evaporation reactor under high vacuum in the order of 10^{-5} Pa on Mo coated soda lime

* Corresponding author at: IRDEP - EDF R&D, 6 quai Watier, BP 49, 78401 Chatou, France.
E-mail address: torben.klinkert@edf.fr (T. Klinkert).

http://dx.doi.org/10.1016/j.tsf.2014.09.074
0040-6090/

glass. The four constituents Cu, In, Ga and Se were evaporated according to a 3-stage process. The deposition rates were controlled by the boat source temperatures, calibrated with a quartz micro-balance. The substrate temperature was set to nominal values of $T_{s,1} = 400$ °C in the first stage and $T_{s,2} = 425$ °C in the 2nd and 3rd stage. Film stoichiometry at the end of stage 2 is determined by end-point detection (described e.g. in [11]) using the temperature signal measured by a thermocouple very close to the back side of the sample. Immediately after the absorber deposition, each sample was cut into two pieces and the CdS and Zn(S,O) buffer layers were deposited by chemical bath deposition.

2.2. Buffer and window layer fabrication and post deposition treatments

The CdS buffer layer was fabricated by chemical bath deposition (CBD) at 60 °C using a classical solution containing thiourea ($SC(NH_2)_2$) as sulfur precursor, ammonium (NH_4OH) as complexing agent and cadmium acetate as Cd donor. The final layer thickness was 50 nm. No post deposition treatments have been conducted and the stack was completed by a sputtered i-ZnO and a ZnO:Al window layer. Solar cells of 0.1 cm^2 were defined by mechanical scribing.

Zn(S,O,OH) films were grown by CBD using thiourea and ammonia as well. In this case, zinc sulfate ($ZnSO_4$) was used as zinc donor. The formulation for the Zn(S,O,OH) bath is $[SC(NH_2)_2] = 0.65$ M, $[ZnSO_4] = 0.15$ M, $[NH_3] = 2$ M with a deposition temperature of 80 °C. After Zn(S,O,OH) deposition, the samples were rinsed in NH_3 solution followed by de-ionized water in order to avoid $Zn(OH)_2$ post-precipitation at the surface of the films. The stack was completed with sputtered window layers of $Zn_{0.75}Mg_{0.25}O$ and ZnO:Al. It has been shown in [12] that the replacement of i-ZnO by $Zn_{0.75}Mg_{0.25}O$ has highly beneficial effects on the open circuit voltage and cell performance as well as on the stability. As for the CdS buffer layer, solar cells of 0.1 cm^2 were defined by mechanical scribing. In order to reduce meta-stabilities of the cells, samples were annealed in air for 10 min at 200 °C and light-soaked for 1 h before current voltage measurements.

2.3. Material and device characterization

GD-OES has been conducted at bare absorber layers without any post-deposition treatments and was quantified using inductively coupled plasma atomic emission spectroscopy. Current–voltage (I–V) measurements of all samples were conducted under standard test conditions (STC) with an AAA solar simulator. For the cells with a Zn(S,O) buffer layer, a light-soaking prior to the I–V measurements was conducted during 1 h under STC. Raman spectroscopy measurements were performed using a Horiba Jobin Yvon LabRam instrument with a 532 nm laser and an ×100 objective.

3. Results

The [Ga] / ([Ga] + [In]) composition profiles as measured by GD-OES are shown in Fig. 1 together with the global compositions [Ga] / ([Ga] + [In]) (CGI) and [Ga] / ([Ga] + [In]) (*GGI*) as well as the band gap energy $E_{g,f}$ at the hetero-interface and the minimum band gap energy $E_{g,\min}$. The band gap was calculated from the GGI using the formula $E_g = 1.0 + 0.65 \cdot GGI + b \cdot GGI \cdot (GGI - 1)$ [13] with a bowing factor $b = 0.1$.

It can be seen that the systematic variation of the Ga and In deposition rates in the 3rd stage of our 3-stage co-evaporation process led to a systematic variation of the [Ga] / ([Ga] + [In]) ratio x_f in the top 400 nm. The composition in the bulk and towards the back-side stays rather constant. Slight GGI variations in this region are inferior to 7% absolute (GGI ≈ 0.47 for $x_f = 0.5$ and GGI ≈ 0.40 for $x_f = 0.45$ at a vertical position of $z = 1.25$ μm). These variations are not systematically related to x_f and attributed to small deviations of the deposition rates in the 1st stage (assuming sticking coefficients of 1, deposition rates of 8.3 nm/min for In and 3.7 nm/min for Ga would lead to a GGI of 0.34 while 7.7 nm/min for In and 4.3 nm/min would lead to a GGI of 0.4). The integral GGI varies slightly due to the front Ga gradient while all samples are overall Cu poor (CGI < 1), as expected for CIGS from a 3-stage process. The variation of the integral CGI between 0.75 and 0.89 is attributed to the non-perfect control of the Cu deposition rate and accidental variations in the 2nd stage. We do not interpret the low Cu content for the highest x_f of 0.59 as a result of the high Ga content and point out that the sample with the second highest x_f of 0.5 has a relatively high CGI of 0.88.

In Fig 2, Raman scattering spectra performed at finished cells of all samples are shown. As described in earlier work [14], a typical CIGS absorption coefficient $\propto = 1.35 \times 10^5$ cm^{-1} [15] for light with a wavelength of 532 nm leads to an absorption of about 99% of the initial photons in the top 170 nm, Raman scattering is thus sensitive to the front region of the CIGS layer.

For each x_f, the curves of cells with a CdS and a Zn(S,O) buffer layer superpose very well. For the samples with a CdS buffer layer, an additional peak at about 305 cm^{-1} is visible, in the literature identified as the first order LO phonon line of CdS [16,17]. The A1-mode of α-Cu(In,Ga)Se_2 is the dominating peak for all samples. As expected, its position successively shifts to higher wave numbers with increasing Ga content from 174.52 cm^{-1} for $x_f = 0.16$ to 178.59 cm^{-1} for $x_f = 0.59$. The shoulder-like shape at 150–170 cm^{-1}, attributed to ordered vacancy

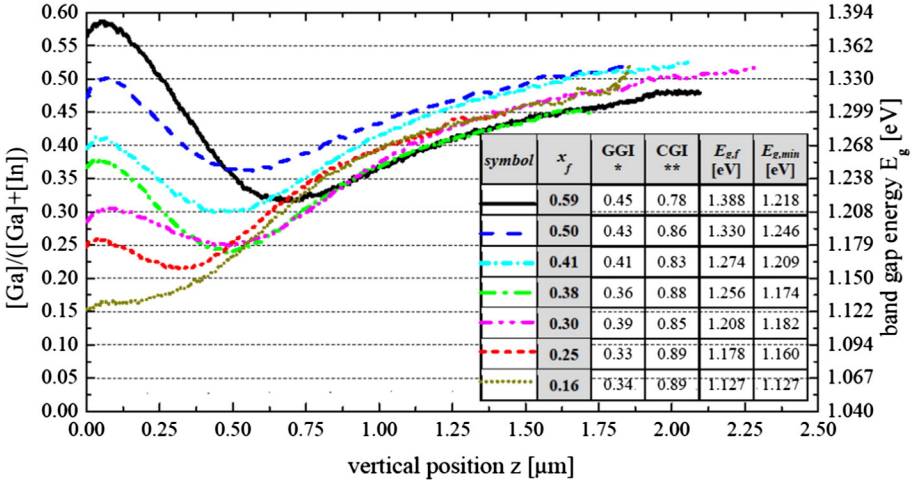

Fig 1. In-depth profiles of the [Ga] / ([Ga] + [In]) compositional ratio measured by GD-OES. The main variation is confined to about the top 400 nm and due to a variation of the In and Ga deposition rates in the 3rd stage of our 3-stage co-evaporation process. (For interpretation of the references to colour in this figure, the reader is referred to the web version of this article.)

Please cite this article as: T. Klinkert, et al., Adaptation of the surface-near Ga content in co-evaporated Cu(In,Ga)Se_2 for CdS versus Zn(S,O)-based buffer layers, Thin Solid Films (2014), http://dx.doi.org/10.1016/j.tsf.2014.09.074